Free Radical Biology and Medicine xxx (xxxx) xxx–xxx

Contents lists available at ScienceDirect

Free Radical Biology and Medicine

journal homepage: www.elsevier.com/locate/freeradbiomed

Short-chain lipid peroxidation products form covalent adducts with pyruvate kinase and inhibit its activity *in vitro* and in breast cancer cells

Bebiana C. Sousa[a], Tanzim Ahmed[a], William L. Dann[a], Jed Ashman[a], Alexandre Guy[b], Thierry Durand[b], Andrew R. Pitt[a], Corinne M. Spickett[a,*]

[a] School of Life and Health Sciences, Aston Triangle, Aston University, B4 7ET, Birmingham, UK
[b] Institut des Biomolécules Max Mousseron (IBMM), UMR 5247, Université de Montpellier, CNRS, ENSCM, Montpellier, France

ARTICLE INFO

Keywords:
Acrolein
4-Hydroxy-2-hexenal
Lipoxidation
Malondialdehyde
Mass spectrometry
Warburg effect

ABSTRACT

Pyruvate kinase catalyses the last step in glycolysis and has been suggested to contribute to the regulation of aerobic glycolysis in cancer cells. It can be inhibited by oxidation of cysteine residues *in vitro* and *in vivo*, which is relevant to the more pro-oxidant state in cancer and proliferating tissues. These conditions also favour lipid peroxidation and the formation of electrophilic fragmentation products, including short-chain aldehydes that can covalently modify proteins. However, as yet few studies have investigated their interactions with pyruvate kinase, so we investigated the effects of three different aldehydes, acrolein, malondialdehyde and 4-hydroxy-2*(E)*-hexenal (HHE), on the structure and activity of the enzyme. Analysis by LC-MS/MS showed unique modification profiles for each aldehyde, but Cys152, Cys423 and Cys474 were the residues most susceptible to electrophilic modification. Analysis of enzymatic activity under these conditions showed that acrolein was the strongest inhibitor, and at incubation times longer than 2 h, pathophysiological concentrations induced significant effects. Treatment of MCF-7 cells with the aldehydes caused similar losses of pyruvate kinase activity to those observed *in vitro*, and at lower concentrations than those required to cause cell death, with time and dose-dependent effects; acrolein adducts on Cys152 and Cys358 were detected. Cys358 and Cys474 are located at or near the allosteric or active sites, and formation of adducts on these residues probably contributes to loss of activity at low treatment concentrations. This study provides the first detailed analysis of the structure-activity relationship of C3 and C6 aldehydes with pyruvate kinase, and suggests that reactive short-chain aldehydes generated in diseases with an oxidative aetiology or from environmental exposure such as smoking could be involved in the metabolic alterations observed in cancer cells, through alteration of pyruvate kinase activity.

1. Introduction

The regulation of glycolysis is extremely important for the flux of metabolites required by cells under different cellular conditions, and highly proliferating cells, such as in tumors or bone marrow, show upregulation of aerobic glycolysis, also known as the Warburg effect [1,2]. Tumour cells are known to have altered redox balance, with higher cellular levels of reactive oxygen species, but also increased antioxidant concentrations or activities [2,3], and this pro-oxidative status is thought to be a requirement for their proliferative state, through alterations in cell signaling pathways and metabolic reprogramming [3,4]. This may be achieved in part through redox modulation of enzymatic activities, as various enzymes in glycolysis are known to be sensitive to cellular redox balance, of which glyceraldehyde-3-phosphate dehydrogenase (GAPDH), pyruvate kinase M2 (PKM2), and phosphofructokinase (PFK) are the most recognized [5]. GAPDH contains a redox-sensitive cysteine in its catalytic site, oxidation of which leads to direct inhibition of its activity [6-8]. It has also been reported that under oxidative stress conditions, PFK can be regulated by oxidative modifications of PFKFB3, which modulates the level of the allosteric activator fructose-2,6-bisphosphate. PFKFB3 can be S-glutathionylated on Cys206, which is located near the substrate binding pocket and causes decreased catalytic activity [9].

The last enzyme of glycolysis, pyruvate kinase, catalyses the conversion of phosphoenolpyruvate and ADP to pyruvate and ATP. It is considered to be a key player in the Warburg effect as it has been observed that tumours and other rapidly proliferating cells contain much higher expression of the PKM2 isoform, which is subject to allosteric regulation and has lower activity compared to the highly active non-allosteric PKM1 isoform that is found in the majority of adult tissues

* Corresponding author. School of Life and Health Sciences, Aston University, Aston Triangle, Birmingham, B4 7ET, UK.
E-mail address: c.m.spickett@aston.ac.uk (C.M. Spickett).

https://doi.org/10.1016/j.freeradbiomed.2019.05.028
Received 3 March 2019; Received in revised form 10 May 2019; Accepted 27 May 2019

[10,11]. PKM1 exists constitutively in the active, tetrameric form, whereas PKM2 occurs in an equilibrium between monomer, dimer and tetramer that can be influenced by the presence of a wide variety of regulators [10]. For example, its activity is activated by the upstream glycolytic metabolite fructose-1,6-bisphosphate (F-1,6-bP), which stabilizes the tetramer, and in the absence of F-1,6-bP its activity drops to 4% [12-14]. Pyruvate kinase can also be inhibited by oxidants such as H_2O_2, as it contains cysteine residues that are susceptible to oxidation, for example Cys358, but the enzymatic activity can be recovered with a reducing agent, demonstrating that inhibition is reversible [13,15,16]. Their oxidation can affect substrate binding, binding of allosteric regulators, or multimerization [17]. Consequently, oxidation has been suggested as a mechanism for inhibiting pyruvate kinase, for example in lung cancer cells [15]. Although a strong dependence on glycolysis for proliferating cells appears to be important, it has been proposed that inhibition of pyruvate kinase during oxidative stress leads to rerouting of glycolytic intermediates into the pentose phosphate pathway in order to generate NADPH and maintain reduced glutathione levels, facilitating cell survival when partially reduced oxygen species (PROS) accumulate [18]. Studies in the eukaryotic model *Saccharomyces cerevisiae* indicate that the build-up of PEP inhibits triose phosphate isomerase and acts as a feedback loop to stimulate the pentose phosphate pathway [19]. Such changes allow cancer cells to meet the increased biosynthetic demands for antioxidants, lipids and nucleotides, promoting tumour growth [11,20].

While it is clear that redox imbalance and increased production of certain oxidants such as hydrogen peroxide or peroxynitrite can affect glycolytic enzymes directly, more reactive compounds such as hydroxyl radicals can also damage other cellular components and cause lipid peroxidation. The peroxidation of lipids containing polyunsaturated fatty acids results in a wide range of reactive products, including short-chain aldehydes that are reactive and can cause covalent modifications of proteins [21,22]. This type of secondary damage is known as lipoxidation and can occur via Schiff's base formation with lysine residues or formation of Michael adducts on histidine, cysteine or lysine residues [23,24]. It has been shown to occur both *in vitro* and *in vivo*, and lipoxidation products have been found in several inflammatory diseases, including atherosclerosis and Alzheimer's disease [24]. Much attention has focused on the lipid peroxidation product 4-hydroxynonenal (HNE), which is often described as the most toxic aldehyde from this source [25], owing to its high reactivity and potential for crosslinking, but a variety of other products deserve consideration. The 6-carbon analogue 4-hydroxyhexenal (HHE) is one of the major lipid peroxidation products of ω-3 PUFAs; it has very comparable reactivity to HNE, and therefore potential importance in disease [26]. The 3-carbon compound malondialdehyde (MDA) is the most studied aldehyde [27] and in parallel with HNE is commonly used as marker of oxidative stress [28], although it should be noted that many of these studies used the TBARS assay, which is not specific for malondialdehyde and is widely considered to be unreliable as an assay for endogenous oxidative stress [29]. It is also bifunctional and has the potential to crosslink proteins [30]. Acrolein is a 3-carbon alkenal more commonly associated with tobacco smoke and processed foods [31], but it may also occur as a breakdown product of lipid peroxidation [32]. It is highly reactive, especially with thiol groups of proteins, and it has been associated apoptosis and disruption of inflammation and antioxidant defence regulation [33,34].

Interestingly, HNE has been suggested to have both pro-tumorigenic and anti-cancer effects. There is substantial evidence that many tumor tissues contain increased levels of HNE adducts with proteins and DNA, and HNE is thought to be both mutagenic and carcinogenic [35]. In contrast, low levels of HNE have been reported to inhibit cell proliferation and angiogenesis as well as inducing differentiation and apoptosis in tumor cell lines [36]. Despite these links between lipoxidation and cancer, as yet relatively little work has been done to study the potential effects of lipid peroxidation-derived aldehydes on glycolytic enzymes involved in the Warburg effect. GAPDH has been investigated because the redox active catalytic cysteine appears to be particularly susceptible to lipoxidation; it has been reported to be modified by HNE *in vitro* [37] and by acrolein in mouse carcinoma cells treated in culture [38]. Interestingly, such modifications were found to cause aggregation, alter the subcellular localization of GAPDH and induce some of its “moonlighting” functions [39,40]. In another study, the sites and mechanism of GAPDH modification by three different α,β-unsaturated carbonyl compounds were compared [41]. In contrast, lipoxidation of pyruvate kinase had been largely unexplored until a recent comparison of the effects of HNE and its di-carbonyl analogue 4-oxononenal (ONE) on PKM2, which demonstrated the potential of these electrophiles to inactivate it [42]. In view of the gap in knowledge on the interactions of short chain reactive alkanals and alkenals with pyruvate kinase, we investigated the modification of this protein by acrolein, malondialdehyde and 4-hydroxyhexanal using LC-MS/MS to map the sites of modification following treatment *in vitro*. We then determined the effects of these treatments on PKM2 activity, both *in vitro* and in the cultured cell line MCF-7, and assessed their impact on cell viability with the aim of determining the potential of different aldehydes reactivity to contribute to metabolic remodelling via PKM2.

2. Materials and methods

2.1. Chemicals

All reagents were purchased from Sigma-Aldrich Chemical Co. (Dorset, UK) unless otherwise indicated. All solvents were of LC-MS grade and ultrapure water (Type 1) was used for buffers and reactions. Formic acid and dithiothreitol (DTT) were purchased from ThermoFisher Scientific (Runcorn, UK).

2.2. Synthesis of 4-hydroxy-2(E)-hexenal

The 4-hydroxy-2(E)-hexenal (HHE) was obtained by cross-metathesis between acrolein and 1-penten-3-ol with Hoveyda-Grubbs catalyst in good yield (68%), following the two published procedures [43,44]. 1H NMR (300 MHz, Acetone-d6) δ 9.57 (d, J = 7.9 Hz, 1H), 6.96 (dd, J = 15.6, 4.4 Hz, 1H), 6.22 (ddd, J = 15.6, 7.9, 1.7 Hz, 1H), 4.32 (ddt, J = 9.5, 6.7, 3.2 Hz, 1H), 4.22 (d, J = 4.9 Hz, 1H), 1.83 – 1.42 (m, 2H), 0.94 (t, J = 7.4 Hz, 3H); 13C NMR (75 MHz, Acetone-d6) δ 193.1, 160.3, 130.3, 71.3, 29.2, 8.9.

2.3. Treatment of pyruvate kinase with aldehydes in vitro

Pyruvate kinase from rabbit muscle (EC2.7.1.40) was prepared at 2.5 mg/mL in phosphate buffer (7 mM sodium phosphate monobasic and 10 mM disodium phosphate dibasic, pH7.4) and treated with acrolein (ACR), malondialdehyde (MDA) (prepared via acid hydrolysis of 1,1,3,3-tetramethoxypropane) or 4-hydroxy-*2(E)*-hexenal (HHE) at 2 μM, 10 μM, 20 μM, 38 μM, 100 μM, 200 μM, 380 μM, 500 μM, 760 μM, 1mM or 5 mM and allowed to react for 10 min, 30 min, 1 h, 2 h or 4 h at 37°C. To stabilize adducts, sodium borohydride ($NaBH_4$) was added to the reaction to a final concentration of 5 mM and left for 30 min at room temperature. This step was omitted when the treated pyruvate kinase was used in the enzymatic activity assay.

2.4. Cell culture and aldehyde treatment

MCF-7 cells were cultured in DMEM (Gibco, UK) supplemented with 10% fetal bovine serum (FBS), 100 U/ml penicillin and 100 μg/ml streptomycin in a humidified incubator at 37°C and 5% CO_2. For each aldehyde treatment, cells were seeded into new flasks at a cell density of 10^6/mL and 10x stock solutions of ACR, MDA or HHE in phosphate buffered containing 0.9% NaCl pH 7.4 were added to the culture media to give final concentrations of 2, 10, 20, 100 or 200 μM and incubated

for 2, 4 or 24 h. Biological triplicates were performed.

2.5. XTT cell viability assay

MCF-7 cells were cultured in a 96-well plate at 10^5 cells per well. The treatments with aldehydes were performed at the concentrations and times described above. XTT [2,3-bis-(2-methoxy-4-nitro-5-sulfophenyl)-2H-tetrazolium-5-carboxanilide] was dissolved in sterile medium to a final concentration of 1 mg/mL. A 10 mM solution PMS (N-methyl dibenzopyrazine methyl sulfate) solution was prepared in phosphate buffer saline (PBS). Immediately prior the start of the assay, 10 µL of PMS was added to 4 mL of XTT solution; 25 µL of PMS/XTT mixture was added to each well and the plate incubated in the dark for 2 h at 37°C before reading the absorbance at 450 nm. The assay was performed with both technical and biological triplicates.

2.6. Cell harvesting, lysis and protein concentration assessment

Cells were harvested using pre-warmed trypsin-EDTA solution followed by centrifugation at 150g for 5 min at 4 °C and lysed in lysis buffer (50 mM Tris-HCl pH 7.5, 1 mM EDTA, 150 mM NaCl, 1% Triton X-100) supplemented immediately prior to usage with cOmplete™ EDTA-free Protease Inhibitor Cocktail (Sigma Aldrich, UK) according to the manufacturer's instructions. After 15 min incubation on ice, the samples were centrifuged at 16,000 g for 2 min and the supernatant (cytosolic extract) was retained. The total protein concentration was determined by the Bradford assay using Pierce™ Coomassie Plus Assay Reagent (ThermoFisher Scientific, UK) in a 96-well plate: 5 µL of sample or standard per well were mixed with 250 µL of Coomassie reagent and after 10 min the absorbance was read at 595 nm. Samples were analysed for enzymatic activity immediately.

2.7. Pyruvate kinase activity assays

Pyruvate kinase activity was measured by a coupled assay using pyruvate-dependent conversion of NADH to NAD^+ by lactate dehydrogenase as the reporter. For analysis of the effects on pyruvate kinase *in vitro*, 5 µL of the aldehyde-treated pyruvate kinase (equivalent to 1U) were added to a cuvette containing 30 µL of 45 mM adenosine 5′-diphosphate (ADP), 30 µL of 45 mM phosphoenolpyruvate (PEP), 30 µL of 6.6 mM β-nicotinamide adenine dinucleotide reduced form (NADH) and 5 µL of 200 U/mL lactate dehydrogenase (LDH) in 900 µL of 50 mM imidazole-HCl buffer pH 7.6, to give a final volume of 1 mL. The reaction at 25 °C was monitored at 340 nm for 10 min and the initial rate of reaction in µmol NADH utilized/min was calculated. For analysis of pyruvate kinase activity following cell treatments, the cytosolic extract was substituted for the commercial pyruvate kinase preparation.

2.8. Protein in-solution digestion

To 100 µL of aldehyde-treated pyruvate kinase prepared as described above, 100 µL of RapiGest SF (Waters, UK) were added and the solution vortexed. DTT was then added to a final concentration of 5 mM and the reaction incubated at 60 °C for 30 min. Cysteine alkylation was then performed by adding iodoacetamide to a final concentration of 15 mM and incubating in the dark for 30 min at room temperature. Trypsin (Trypsin Gold, Mass Spectrometry Grade, Promega, Southampton, UK) was added to a final concentration of 7 µg/mL and the samples were incubated overnight at 37 °C. To prepare samples for LC/MS, trifluoroacetic acid (TFA) was added to a final concentration of 0.5% and the reaction incubated at 37 °C for 45 min, during which time a precipitate formed. Acid-treated samples were centrifuged at 16000 g for 10 min then the supernatant carefully transferred to another tube and dried in a centrifugal evaporator and stored dry at -20 °C. Samples were resuspended in H_2O/acetonitrile (98%/2%), 0.1% formic acid prior to MS analysis.

2.9. Liquid chromatography-tandem mass spectrometry (LC-MS/MS) analysis

Peptides were separated and analysed using an Ultimate 3000 system (Thermo Scientific, Hemel Hemstead, UK) coupled to a 5600 TripleTOF (ABSciex, Warrington, UK). The analysis was performed as previously described [45]. Briefly, the peptide solution was loaded onto a C18 trap column (C18 PepMapTM, 5 µm, 0.5 x 5 mm, Thermo Scientific, Hemel Hemstead, UK) before separation on a nano-HPLC column (C18 PepMapTM, 5 µm, 0.075 x 150 mm, Thermo Scientific, Hemel Hemstead, UK) at 300 nL/min using a gradient elution running from 2% to 45% aqueous acetonitrile, 0.1% formic acid over 45 min. Ionization of the peptides was achieved with the spray voltage set at 2.4 kV, a source temperature of 150°C, declustering potential of 100 V and a curtain gas setting of 25. Survey scans were collected in positive mode from 350 to 2000 Da using high-sensitivity TOF-MS mode. Information-dependent acquisition (IDA) was used to collect MS/MS data using the following criteria: the 10 most intense ions with +2 to +5 charge states and a minimum intensity of 200 cps were chosen for analysis, using dynamic exclusion for 12 s and standard rolling collision energy settings.

2.10. Database searches

The Mascot® probability based search engine (Matrix Science, London, version 2.4.0) was used to interrogate the SwissProt 2019_03 primary database. LC-MS .wiff files of each sample were searched for protein identification and oxidative post-translational modifications (oxPTMs). For protein identification, variable modifications of methionine oxidation and carbamidomethyl cysteine were used. For the analysis of the lipoxidation products, the initial searches additionally used a variable modification list including reduced and unreduced ACR (mass changes of 56.06 Da, 58.08 Da, 40.06 Da, 94.11 Da, 56.06 Da, 76.09 Da), MDA (mass changes of 54.05 Da, 56.06 Da, 134.13 Da, 36.03 Da and 26.04 Da) or HHE (mass changes of 114.14 Da, 93.13 Da, 78.11 Da) adducts at cysteine, lysine and histidine residues. Other parameters for the searches were as follows: Enzyme: Trypsin; Peptide tolerance: ± 0.6 Da; MS/MS tolerance: ± 0.6 Da; Peptide charge state: +2, +3; Max Missed cleavages: 1; #13C: 0; Quantitation: None; Instrument: ESI-QUAD-TOF; Data format: Mascot Generic; Experimental mass values: Monoisotopic; Taxonomy: Chordata. All data identifying modifications were manually validated before inclusion.

2.11. Statistical analysis

Data were analysed with Graph Pad Prism using one-way ANOVA for single time point (Fig. 2 and Suppl. Figure 2) and using two-way ANOVA for multiple time point (Fig. 3 and Fig. 4), both with Dunnett's multiple comparisons test, comparing the values of each treated sample to the mean of the untreated control, normalized to 100%. Data are shown as averages ± SEM.

3. Results

3.1. Identification and mapping of lipoxidation on pyruvate kinase following 10 min treatments

The modification of pyruvate kinase by acrolein, MDA and HHE was investigated using LC-MS/MS to map the sites of modification following treatment *in vitro* at 37 °C for 10 min. Initially the MASCOT® software was used to identify modified peptides, and then each potential modification was confirmed by de novo sequencing of the MS/MS spectrum including detection of diagnostic ions as reported previously [46]; examples of modification by each aldehyde are shown in Suppl. Figures 1 and 2. This approach allowed the identification of 11 peptides modified by acrolein, 10 peptides modified by HHE and 9 peptides modified by

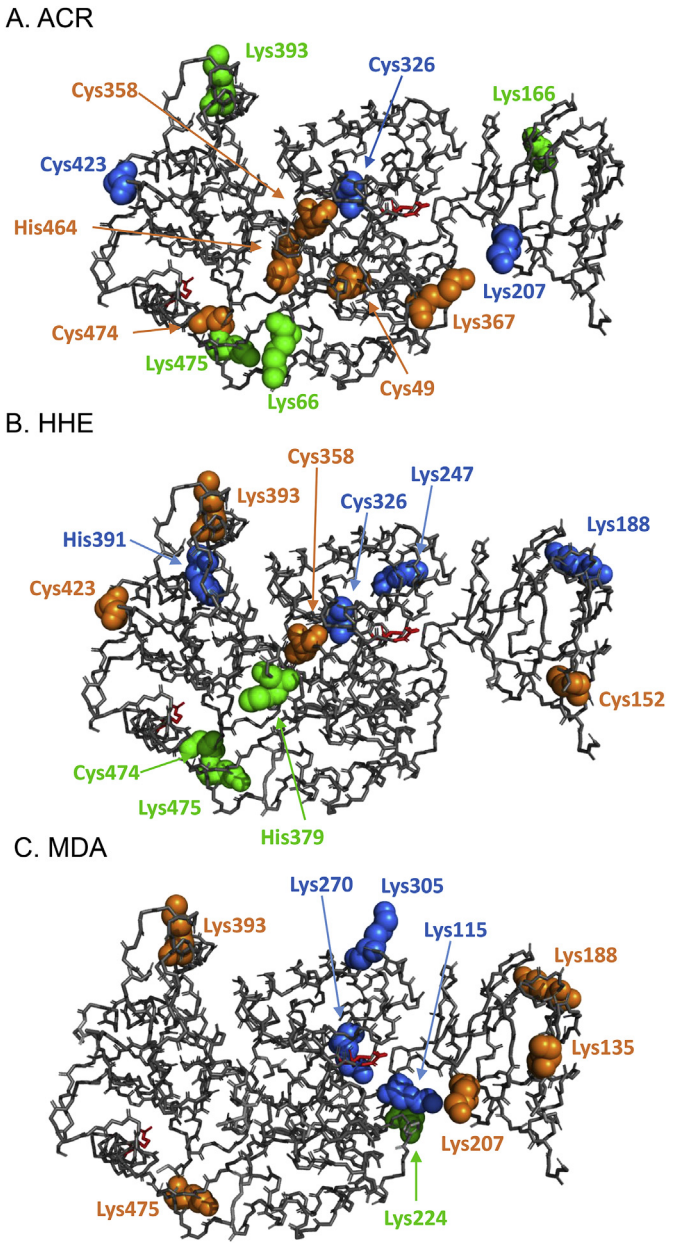

Fig. 1. Mapping of lipoxidation adducts to the crystal structure of pyruvate kinase. Backbone structure with modified residues indicated in space-fill form, showing the location of adducts of acrolein (A), HHE (B) and MDA (C). The modified residues are color-coded with orange indicating those found only at 380 μM, green for those found additionally at 760 μM and blue for ones found additionally at 5 mM. (For interpretation of the references to color in this figure legend, the reader is referred to the Web version of this article.)

MDA based on peptide molecular weight, mass/charge ratio and charge of the peptide ion, MS/MS ion score and LC retention time (Table 1). Acrolein adducts were either Schiff's bases (+40 Da), Michael adducts (+58 Da) or FDP adducts (+96 Da), while for HHE Schiff's bases occurred at +96 Da and Michael adducts at +114 Da; only Schiff's bases (+54 Da) were formed with malondialdehyde. The majority of the identified adducts occurred on lysine and cysteine residues, although some histidine adducts were identified. The position of the modified residues in the enzyme structure is shown in Fig. 1. It can be seen that the susceptibility of residues identified as modified differed substantially between the aldehydes: the profiles of modification were most similar between acrolein and HHE, as would be expected considering that they are both α,β-unsaturated aldehydes, but even so there were

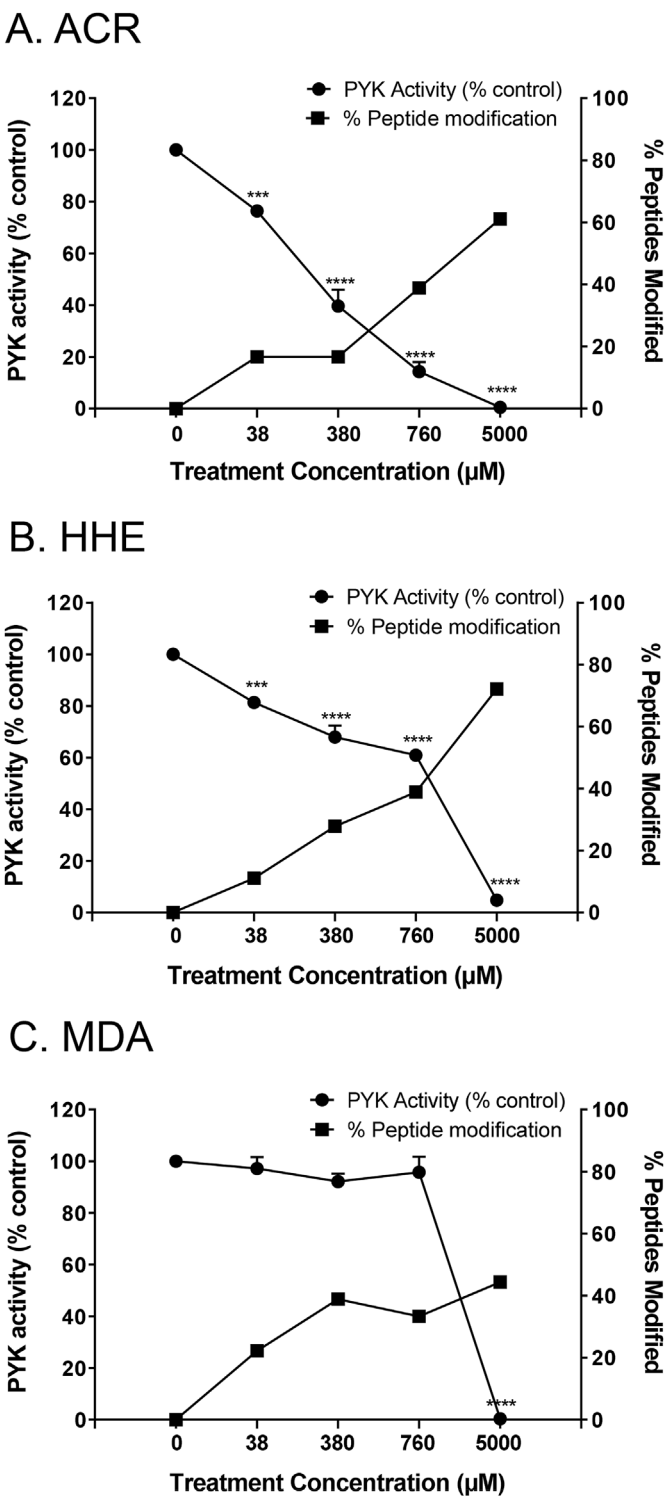

Fig. 2. Inverse relationship of the dose-dependent effect of aldehydes on the activity of pyruvate kinase *in vitro* and the percentage of modified pyruvate kinase peptides identified. Pyruvate kinase (PYK) was treated with 38 μM, 380 μM, 760 μM and 5 mM final concentrations of acrolein, 4-hydroxy-hexenal or malondialdehyde for 10 min before the assessment of its activity by spectrophotometric assay of NADH oxidation at 340 nm (n = 4; Mean ± SEM; *p < 0.1 **p < 0.01 ***p < 0.001 ****p < 0.0001). Peptide modification was determined from the total number of modified peptides as a % of the total modifiable peptides in the sequence.

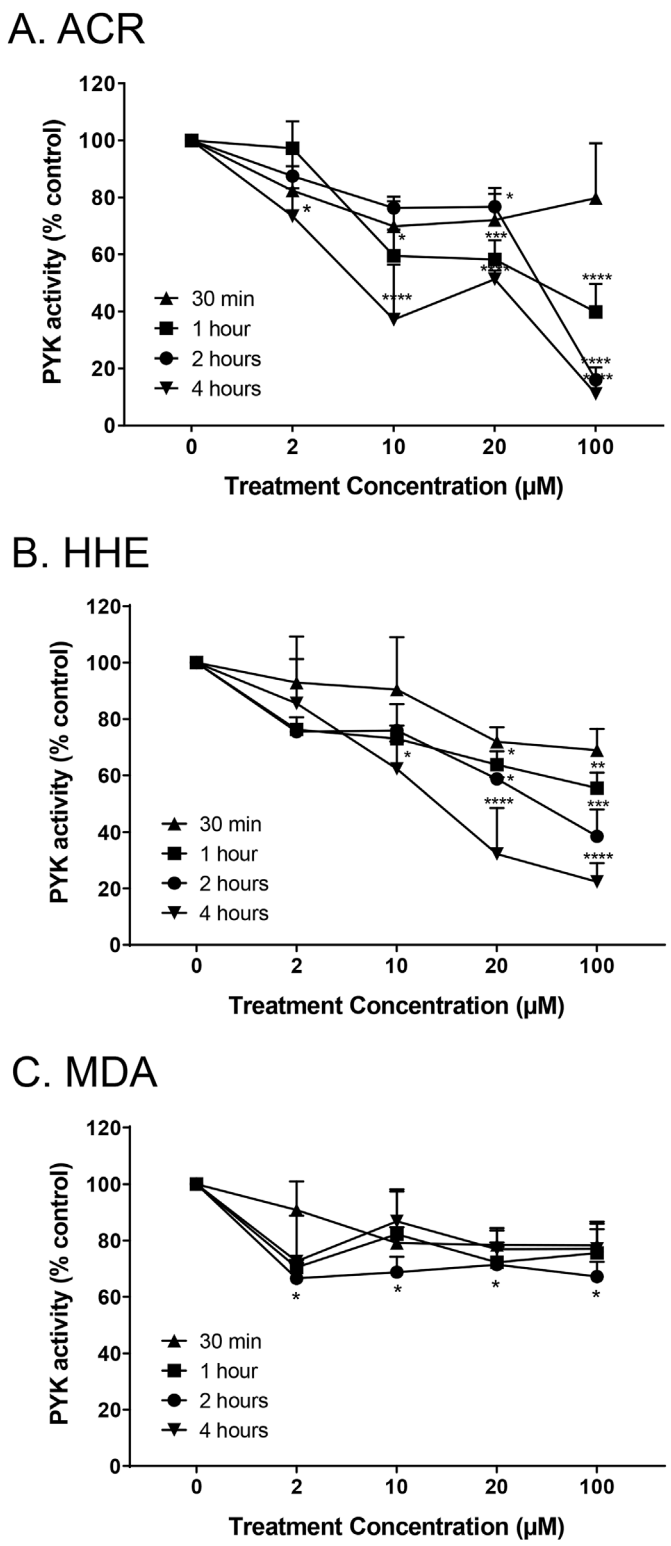

Fig. 3. Effect of longer treatments with acrolein, 4-hydroxy-hexenal and malondialdehyde on the activity of pyruvate kinase *in vitro*. Pyruvate kinase was treated with 2 μM, 10 μM, 20 μM and 100 μM of each aldehyde for 30 min, 1 h, 2 h or 4 h before the assessment of its activity (n = 3; Mean ± SEM; *p < 0.1 **p < 0.01, ***p < 0.001 and ****p < 0.0001).

clear differences (e.g. HHE formed adducts on C152, K188, K247, H379 that were not detected with acrolein, whereas acrolein modified K66, K166, K207 and H464). MDA gave a rather different profile, as only lysine adducts were formed and modifications on K115, K224 and K270

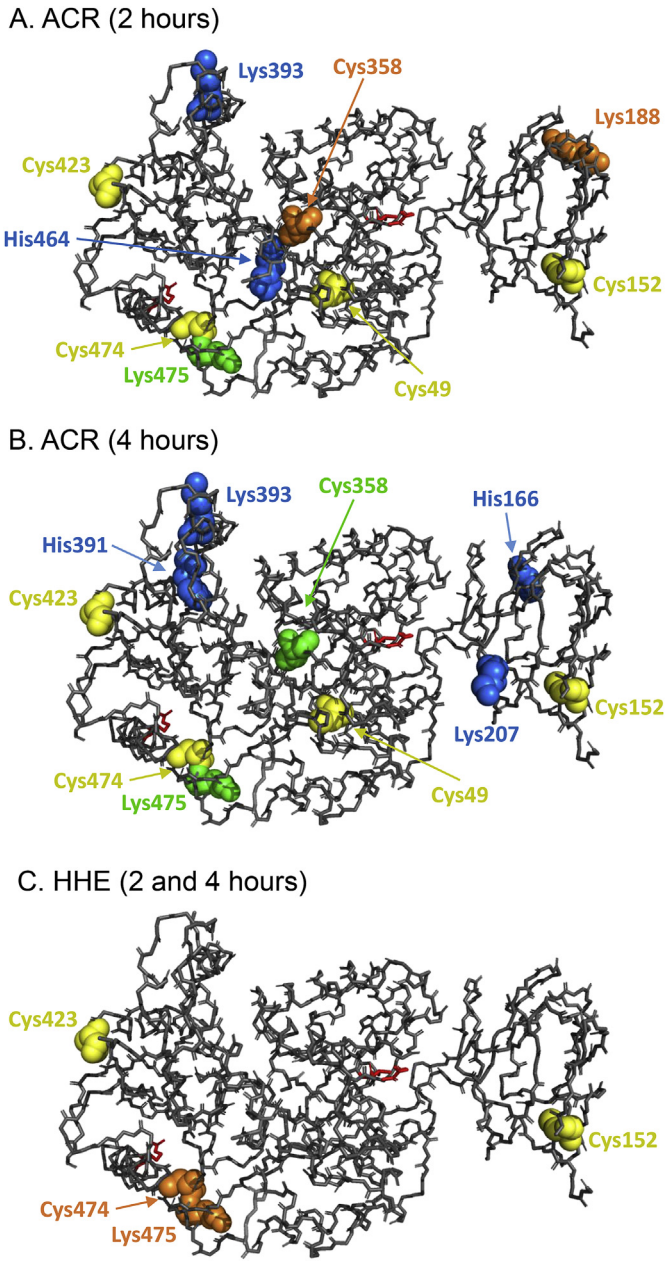

Fig. 4. Mapping of lipoxidation adducts formed at low concentrations for 4 h treatments. Backbone structure with modified residues indicated in space-fill form, showing the location of adducts of acrolein at 2 h (A); acrolein at 4 h (B) and HHE at both time points (C). The modified residues are color-coded with yellow indicating those found only at 10 μM, orange for those found additionally at 20 μM, green for those found additionally at 100 μM and blue for ones found additionally at 200 μM. (For interpretation of the references to color in this figure legend, the reader is referred to the Web version of this article.)

were unique to this aldehyde. Only K393 and K475 were consistently identified by MASCOT as modified by all aldehydes. To investigate further the factors affecting the sites of modification, the modifications were also mapped onto space-filling models that were colour-coded to indicate the hydrophobicity of the location (Suppl. Figure 3), and short videos were prepared to enable clearer 3 dimensional visualization (Suppl. Material Videos 1-3). Overall, it can be seen that there was no clear correlation between the hydrophobicity and site of modification, and a number of modifications observed at lower treatment concentrations occurred at relatively polar sites, either on the surface of the enzyme or in clefts. The most notable observation was that acrolein was

Table 1
Pyruvate kinase residues modified after 10 min treatment at high aldehyde concentrations *in vitro*

Modified Residues	Pyruvate kinase modified peptides ([a][b])	Theoretical mass of modified peptide	Observed mass of modified peptide	*m/z* (charge)	Ion score	Rt (min)	Aldehyde treatment			
							38 μM	380 μM	760 μM	5 mM
Acrolein										
Cys49	$_{44}$NTGII**C**$^{+56}$TIGPASR$_{56}$	1357.70	1357.83	679.9 (2+)	52	27.76	-	-	-	✓
Cys49	$_{44}$NTGII**C**$^{+58}$TIGPASR$_{56}$	1359.72	1359.84	680.9 (2+)	54	27.69	-	✓	✓	✓
Lys66	$_{63}$EMI**K**$^{+58}$SGMNVAR$_{73}$	1292.66	1292.81	431.9 (3+)	16	21.87	-	-	✓	✓
Lys166	$_{163}$NIC*$\mathbf{K}^{+58}$VVDVGSK$_{173}$	1275.68	1275.81	638.9 (2+)	13	21.94	-	-	✓	✓
Lys207	$_{207}\mathbf{K}^{+40}$GVNLPGAAVDLPAVSEK$_{224}$	1804.01	1804.19	602.4 (3+)	62	31.00	-	-	-	✓
Cys326	$_{320}$AGKPVI**C**$^{+58}$ATQMLESMIK$_{336}$	1876.98	1876.17	626.7 (3+)	19	52.72	-	-	-	✓
Cys358	$_{343}$AEGSDVANAVLDGADC^{+58}IMLSGETAK$_{367}$	2494.16	2494.37	832.5 (3+)	37	49.48	✓	-	-	-
Lys367	$_{343}$AEGSDVANAVLDGADC*IMLSGETA**K**$^{+58}$GDYPLEAVR$_{376}$	3551.67	3551.99	889.0 (4+)	26	47.52	-	✓	-	-
Lys393	$_{393}\mathbf{K}^{+58}$LFELAR$_{400}$	1062.61	1062.72	532.4 (2+)	27	29.34	-	-	✓	✓
Lys393	$_{393}\mathbf{K}^{+40}$LFELAR$_{400}$	1060.59	1060.63	531.3 (2+)	9	21.87	-	-	✓	✓
Cys423	$_{423}\mathbf{C}^{+58}$LAAALIVLTESGR$_{436}$	1473.82	1473.96	737.9 (2+)	89	51.53	-	-	-	✓
His464	$_{462}$QA**H**$^{+40}$LYR$_{467}$	826.44	826.51	414.3 (2+)	21	21.03	✓	-	-	-
Cys474	$_{468}$GIFPVV**C**$^{+58}$K$_{475}$	975.55	975.63	460.8 (2+)	31	30.97	✓	✓	✓	✓
Lys475	$_{468}$GIFPVVC*$\mathbf{K}^{+58}$DPVQEAWAEDVDLR$_{489}$	2599.30	2599.51	867.5 (3+)	57	53.72	-	-	✓	✓
4-Hydroxy-hexenal										
Cys152	$_{152}\mathbf{C}^{+96}$DENILWLDYK$_{162}$	1506.71	1506.86	754.44 (2+)	24	39.35	-	✓	✓	✓
Cys152	$_{152}\mathbf{C}^{+114}$DENILWLDYK$_{162}$	1524.72	1524.72	763.43 (2+)	72	33.52	✓	✓	✓	✓
Lys188	$_{187}$Q**K**$^{+114}$GPDFLVTEVENGGFLGSK$_{206}$	2235.14	2235.34	746.12 (3+)	17	35.84	-	-	-	✓
Lys247	$_{247}\mathbf{K}^{+96}$AADVHEVR$_{255}$	1119.60	1119.73	374.25 (3+)	27	18.23	-	-	-	✓
Cys326	$_{320}$AGKPVI**C**$^{+96}$ATQMLESMIKKPRPTR$_{342}$	2650.45	2650.72	531.15 (5+)	14	38.00	-	-	-	✓
Cys326	$_{320}$AGKPVI**C**$^{+114}$ATQMLESMIKKPRPTR$_{342}$	2668.46	2668.72	445.79 (6+)	13	29.35	-	-	-	✓
Cys358	$_{343}$AEGSDVANAVLDGADC^{+114}IMLSGETAK$_{367}$	2550.18	2550.42	851.15 (3+)	36	36.37	-	✓	✓	✓
His379	$_{377}$MQ**H**$^{+114}$LIAR$_{383}$	981.54	981.64	491.83 (2+)	13	19.81	-	-	✓	✓
His391	$_{384}$EAEAAMF**H**$^{+114}$R$_{392}$	1174.54	1174.67	392.56 (3+)	10	21.82	-	-	-	✓
Lys393	$_{393}\mathbf{K}^{+114}$LFEELAR$_{400}$	1118.63	1118.72	560.37 (2+)	26	29.38	-	✓	✓	✓
Cys423	$_{423}\mathbf{C}^{+96}$LAAALIVLTESGR$_{436}$	1529.85	1529.98	765.99 (2+)	76	40.94	✓	✓	✓	✓
Cys474	$_{468}$GIFPVV**C**$^{+114}$K$_{475}$	975.55	975.62	488.82 (2+)	26	28.22	-	-	✓	✓
Lys475	$_{468}$GIFPVVC**K**$^{+114}$DPVQEAWAEDVDLR$_{489}$	2599.29	2599.49	867.50 (3+)	85	33.83	-	-	-	✓
Malondialdehyde										
Lys115	$_{93}$TATESFASDPILYRPVAVALDT**K**$^{+54}$GPEIR$_{120}$	3070.59	3070.81	768.71 (4+)	42	34.07	-	✓	-	✓
Lys135	$_{126}$GSGTAEVEL**K**$^{+54}$K$_{136}$	1171.61	1171.52	391.51 (3+)	52	18.74	-	✓	✓	-
Lys188	$_{187}$Q**K**$^{+54}$GPDFLVTEVENGGFLGSK$_{206}$	2175.08	2175.21	726.08 (3+)	94	34.69	✓	✓	✓	✓
Lys207	$_{207}\mathbf{K}^{+54}$GVNLPGAAVDLPAVSEK$_{224}$	1817.99	1818.03	607.02 (3+)	70	28.67	✓	✓	✓	✓
Lys224	$_{208}$GVNLPGAAVDLPAVSE**K**$^{+54}$DIQDLK$_{230}$	2402.27	2402.45	801.82 (3+)	87	33.97	-	✓	✓	✓
Lys270	$_{267}$IIS**K**$^{+54}$IENHEGVR$_{278}$	1447.78	1447.74	483.59 (3+)	82	23.05	-	-	-	✓
Lys305	$_{295}$GDLGIEIPAEK^{+54}VFLAQK$_{311}$	1881.03	1881.08	628.03 (3+)	48	34.80	-	-	-	✓
Lys393	$_{393}\mathbf{K}^{+54}$LFEELAR$_{400}$	1058.58	1058.57	530.29 (2+)	37	27.85	✓	✓	✓	✓
Lys475	$_{468}$GIFPVVC*$\mathbf{K}^{+54}$DPVQEAWAEDVDLR$_{489}$	2596.26	2596.49	866.50 (3+)	72	36.79	✓	✓	✓	✓

[a] (subscript) – amino acid position in the mature protein.
[b] (superscript) - mass difference corresponding to the modification.

able to penetrate more readily into narrow pockets in the enzyme, compared to HHE.

3.2. Inhibition of pyruvate kinase activity following treatment in vitro

The effect of the same treatment time and concentrations on pyruvate kinase activity were determined *in vitro* by a coupled spectrophotometric assay. All acrolein and HHE treatments had a significant dose-dependent effect on the enzymatic activity, while MDA treatments at lower concentration had no effect and a decrease in activity was only observed at the highest concentration of 5 mM (Fig. 2). The number of modified peptides detected as a percentage of the total number of modifiable tryptic peptides in the protein are shown in Fig. 2 and a clear inverse relationship between activity and modification can be seen. HHE gave the highest maximum number of modified peptides, followed by acrolein, and MDA was the lowest, reflecting the fact that only lysine residues can be modified by this aldehyde. However, at 380 μM treatment, MDA actually gave a higher percentage of modified peptides than the other two aldehydes. Subsequently, the effects of a wider range of treatment concentrations that included physiological (2 μM) to pathophysiological (20-100 μM) concentrations on pyruvate kinase activity were tested (Suppl. Figure 4). It can be seen that acrolein caused a dose-dependent decrease in the activity of pyruvate kinase, with 70% activity at 100 μM and 200 μM, 40% at 500 μM and 10% at 1 mM treatment, corresponding to substantially more inhibition than either of the other aldehydes.

3.3. Effect of longer treatment times on activity and lipoxidation of pyruvate kinase

It was noted that the treatment concentrations required to cause significant inhibition were extremely high, and it was hypothesized that this might relate to the very short incubation times tested initially, despite the fact that the reaction of acrolein with protein was expected to be rapid. Therefore, further experiments were carried out with longer incubations of 30 min to 4 h with the lower range of concentrations for each aldehyde (Fig. 3). Both acrolein and HHE showed a general time-dependent trend, with longer incubations showing more extensive inhibition of activity. After 1 h reaction with acrolein, significant effects on the activity were observed above 10 μM, with only 40% activity remaining in the 100 μM treatment. A 2 h incubation caused a decrease in activity to approximately 20% at treatment concentrations of 100μM or greater, and further inhibition was observed after 4 h reaction with 40% activity remaining at 10 μM, a known pathophysiological

Table 2
Pyruvate kinase residues modified after 4 h treatment with low concentrations of aldehydes.

Modified Residues	Pyruvate kinase modified peptides[ab]	Theoretical mass of modified peptide	Observed mass of modified peptide	*m/z* (charge)	Ion score	Rt (min)	Aldehyde treatment (4 h)				
							2 μM	10 μM	20 μM	100 μM	200 μM
Acrolein											
Cys49	$_{44}$NTGII**C**$^{+58}$TIGPASR$_{56}$	1359.72	1359.61	680.81 (2+)	80	15.97	-	✓	✓	✓	✓
Cys152	$_{152}$**C**$^{+58}$DENILWLDYK$_{162}$	1468.69	1468.58	735.29 (2+)	91	19.57	✓	✓	✓	✓	✓
Lys166	$_{163}$NIC*K^{+58}VVDVGSK$_{173}$	1275.68	1275.57	426.19 (3+)	26	11.56	-	-	-	-	✓
Lys207	$_{207}$**K**$^{+58}$GVNLPGAAVDLPAVSEK$_{224}$	1822.02	1821.83	608.28 (3+)	16	16.21	-	-	-	-	✓
Lys207	$_{207}$**K**$^{+96}$GVNLPGAAVDLPAVSEK$_{224}$	1860.04	1859.89	620.97 (3+)	44	16.47	-	-	-	-	✓
Cys358	$_{343}$AEGSDVANAVLDGAD**C**$^{+58}$IMLSGETAK$_{367}$	2494.16	2493.97	832.33 (3+)	118	21.22	-	-	-	✓	✓
His391	$_{384}$EAEAAMF**H**$^{+58}$R$_{392}$	1118.52	1118.41	373.81 (3+)	46	11.64	-	-	-	-	✓
Lys393	$_{393}$**K**$^{+58}$LFELAR$_{400}$	1062.61	1062.51	355.18 (3+)	37	14.66	-	-	-	-	✓
Lys393	$_{393}$**K**$^{+96}$LFELAR$_{400}$	1100.62	1100.52	367.84 (3+)	39	14.83	-	-	-	-	✓
Cys423	$_{423}$**C**$^{+58}$LAAALIVLTESGR$_{436}$	1473.82	1473.71	737.86 (2+)	108	20.72	-	✓	✓	✓	✓
Cys474	$_{468}$GIFPVV**C**$^{+58}$K$_{475}$	919.52	919.44	460.72 (2+)	47	17.13	-	✓	✓	✓	✓
Lys475	$_{468}$GIFPVVC*K^{+58}DPVQEAWAEDVDLR$_{489}$	2543.27	2543.10	848.71 (3+)	103	19.99	-	-	-	✓	✓
4-Hydroxy-2-hexenal											
Cys152	$_{152}$**C**$^{+96}$DENILWLDYK$_{162}$	1506.71	1506.61	754.31 (2+)	18	22.46	-	-	-	-	✓
Cys152	$_{152}$**C**$^{+114}$DENILWLDYK$_{162}$	1524.72	1524.59	763.30 (2+)	46	20.12	✓	✓	✓	✓	✓
Cys423	$_{423}$**C**$^{+114}$LAAALIVLTESGR$_{436}$	1529.85	1529.72	765.87 (2+)	77	22.37	✓	✓	✓	✓	✓
Cys474	$_{468}$GIFPVV**C**$^{+114}$K$_{475}$	975.55	975.44	488.73 (2+)	26	16.76	-	-	✓	✓	✓
Lys475	$_{468}$GIFPVVC**K**$^{+114}$DPVQEAWAEDVDLR$_{489}$	2599.29	2599.11	867.38 (3+)	91	18.97	-	-	✓	✓	✓
Malondialdehyde											
	No modifications detected										

[a] (subscript) – amino acid position in the mature protein.
[b] (superscript) - mass difference corresponding to the modification.

concentration [47,48] and 20% at 100 μM. In the case of HHE, at a treatment concentration of 100 μM the effect on the activity of pyruvate kinase was time-dependent, with 70% remaining after 30 min, 55% after 1 h, 40% after 2 h and 30% after 4 h. Comparing the two aldehydes, acrolein appeared to cause more inhibition. Unlike the α,β-unsaturated aldehydes, MDA did not show a clear dose or time-dependent effect on the activity of pyruvate kinase, although significant inhibition was observed at all concentrations following a 2 h treatment. LC-MS/MS analysis of the modified pyruvate kinase after 4 h allowed the identification of 10 peptides modified by acrolein and 4 peptides modified by HHE (Table 2). Mostly the same adducts were observed after 2 h (Suppl. Table 1), except that Lys166, Lys207 and His391 were only found at 4 h, and Lys188 and His464 were only found at 2 h. All the amino acid residues found to be modified with the longer and lower treatments were ones that were modified after short high concentration treatments with acrolein and HHE, but no MDA adducts could be detected. As at the shorter treatment times, there was an inverse relationship between enzyme activity and % of peptides modified, although the total level of modification was much lower for these treatment concentrations (Suppl. Fig. 5). The sites of modifications were mapped to the 3D crystal structure, and are shown in Fig. 4; it can be seen that cysteine residues were the most sensitive to adduct formation with both acrolein and HHE. Suppl. Fig. 6 and Suppl. Material Videos 4-6 show the hydrophobicity of these sites, and support the lack of obvious correlation noted above.

3.4. Comparison of aldehyde effects on MCF-7 cell pyruvate kinase activity and cell viability

To investigate the ability of the aldehydes to cause inhibition of pyruvate kinase in a cellular environment, MCF-7 cells were treated in culture with aldehydes and their impact on extractable pyruvate kinase activity and cell viability was tested. Cells were treated with the same acrolein, MDA and HHE concentrations as above for 2 h or 24 h (Fig. 5). Two hour treatments at 10 μM acrolein inhibited the activity of pyruvate kinase to 20% of control (**A**), while higher concentration treatments had an even more severe effect on the activity of the enzyme. Interestingly, cellular pyruvate kinase activity seemed to be less sensitive to 24-h acrolein treatment with 2-10 μM acrolein, although at higher concentrations the effect was very similar to 2 h. In contrast, the cell viability showed a slightly different response to treatments at the two time points. Neither treatment time with acrolein caused significant loss of cell viability until concentrations of 100 μM, but the higher concentrations were more toxic at 24 h (Fig. 5B). HHE caused a similar, though more gradual, decrease in the enzymatic activity. The 2 h treatment at 10 μM inhibited the activity of pyruvate kinase to 60% of control (Fig. 5C) and higher concentration treatments caused an even more severe effect. As with acrolein, pyruvate kinase activity seemed to be less sensitive to 24 h HHE treatment at all concentrations. Interestingly, these treatments only caused a maximum of 20% of loss in cell viability (Fig. 5D). A similar, though smaller, effect on cellular pyruvate kinase activity was observed for MDA treatments (Fig. 5E); there was a concentration-dependent loss of pyruvate kinase activity that appeared greater for the 2 h treatment compared to 24 h, but in contrast to acrolein, MDA caused no significant loss of viability at any concentration or either time point (Fig. 5F). Extracts of cells treated with 10 and 200 μM acrolein were also subjected to in-gel digestion and analysed by LC-MS/MS to search for modifications of cellular pyruvate kinase. Although the sequence coverage was low, modifications on Cys152 and Cys358 were detected (Suppl. Table 2 and Suppl. Fig. 7), in agreement with the data from treatments of pyruvate kinase *in vitro*, which suggested that these residues are highly susceptible to adduct formation.

4. Discussion

Pyruvate kinase is an important regulatory enzyme in glycolysis, and changes in its expression level, isoform and activity have been linked to the switch to aerobic glycolysis in cancer and proliferating cells [49]. Cancer cells also have altered redox status [4] leading to increased lipid peroxidation and formation of electrophilic short chain carbonyl species, but previously there have been few studies of their effects on pyruvate kinase. To address this question, we measured the inhibition of pyruvate kinase activity caused by incubation with acrolein, HHE and MDA *in vitro*, and analysed the formation of protein-

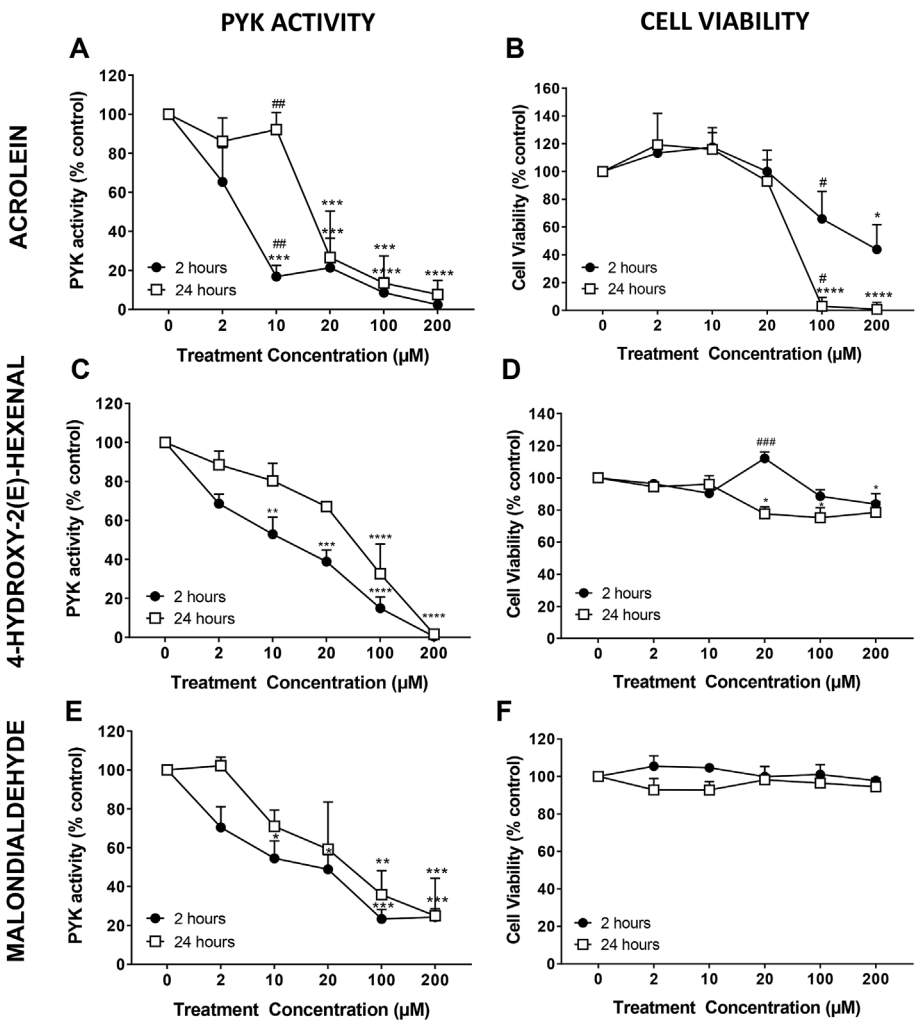

Fig. 5. Dose- and time-dependence of aldehyde treatment on the activity of pyruvate kinase and viability of aldehyde-treated MCF-7 cells. Pyruvate kinase activity is shown on the left for acrolein (A), 4-hydroxyl-2(E)-hexenal (C) and malondialdehyde (E), while cell viability is shown on the right: acrolein (B), 4-hydroxyl-2(E)-hexenal (D) and malondialdehyde (F). Cells were treated with 2 μM, 10 μM, 20 μM, 100 μM and 200 μM of each aldehyde for 2 h or 24 h before proteins were extracted and 10 μg of extract were used for pyruvate kinase activity to be assessed. Cell viability assays were performed with n = 3 for MDA and HHE and n = 4 for ACR (Mean ± SEM; *p < 0.1 **p < 0.01, ***p < 0.001 and ****p < 0.0001). * Comparison between treatments and control for each incubation time. # comparison between incubation times.

aldehyde adducts. There was clearly an inverse relationship between the extent of adduct formation and the activity of the enzyme for all three aldehydes. The data showed that acrolein caused the greatest inhibition of pyruvate kinase, while HHE had an intermediate effect and MDA had no significant effect until much higher concentrations. The lack of inhibition by MDA probably relates to its different chemistry, specifically that it is only able to react with lysines to form Schiff's base adducts, although like the other aldehydes it can cause cross-linking. The mass spectrometry data strongly suggested different profiles of susceptibility of pyruvate kinase residues to the aldehydes. It was also observed that the extent of inhibition was dependent on the length of incubation as well as the treatment concentration, with longer treatments leading to loss of activity at much lower and physiologically relevant concentrations. This demonstrates that the reactions are relatively slow to reach equilibrium and moreover suggests that reversibility of adduct formation is not a significant factor. In cells treated with aldehydes, pyruvate kinase activity was lost at slightly lower concentrations than for the treatment *in vitro*, and did not correlate with loss of cell viability until the highest treatment concentrations, indicating that the enzymatic effect was not simply due to general cell dysfunction. Interestingly, it has been reported previously that tumour cells can survive and proliferate with very low pyruvate kinase activity [50].

The variation in residue susceptibility to the three aldehydes was notable. Even with acrolein and HHE, which are both α,β-alkenals that can form Michael adducts with cysteine and histidine, although there were six common modified residues (Cys326, Cys358, Lys393, Cys423, Cys474, Lys475) following short treatments at higher concentrations, there were also several differences. This may be a result of the smaller size of acrolein and a corresponding ability to access more buried residues, such as Cys49, Lys207 and His464. This was apparent from the video clips of the space filling models. Some additional residues modified by HHE seemed to be surface accessible, including Lys188 and Lys247, so it is unclear why these were not adducted by acrolein; mapping of the surface hydrophobicity did not suggest that it correlated strongly to this factor. The only overlap between MDA modifications and both other aldehydes was in adducts on Lys393 and Lys475, while at lower concentrations no modifications by MDA were detected. It is important to note that other modifications might have been present in the proteins, but were not identified by the Mascot searches, for example due to cross-linking; however, it is likely that any other modifications were of relatively low abundance.

Consideration of the differences in sites of modification is important to understand the functional effects induced. Two of the cysteine residues found modified by acrolein and HHE have been previously reported to be modified by oxidation [17] or electrophilic attack by HNE and ONE [42]. Cys326 is buried in the tetramer but accessible in the monomeric form and a modification at this site could prevent the reformation of the active tetrameric form of pyruvate kinase [17], or destabilize the tetramer. However, in our experiments, this residue was only observed to be modified at very high treatment concentrations, probably reflecting the fact that in the tetrameric PKM1 form it is protected. In contrast, Cys358 was susceptible to lipoxidation at lower concentrations, although it was not the most susceptible site. This

residue is located close to the substrate binding site and has previously been reported to regulate pyruvate kinase activity by oxidation, promoting optimal conditions for tumor growth and survival under oxidative stress, and substitution of Cys358 by Ser358 protected PKM2 from oxidant-induced inhibition by stabilizing the tetrameric form [15]. Acetylation of K305 had been reported to reduce pyruvate kinase activity by lowering the affinity to PEP or triggering the degradation of the enzyme itself under nutrient-depleted conditions [51], but was only modified at the highest MDA treatment. Cys424 in PKM2 is thought to play a role in protein-protein interactions and allosteric regulation by F-1,6-bP, and has been reported to be modified by electrophilic carbonyl species [42]; this residue is not present in PKM1 but Cys423 is also located at the subunit interface and it is conceivable that its modification can destabilize the tetrameric form. Cys423 was one of the most sensitive residues, showing adduct formation at 10 μM acrolein and HHE, together with Cys152. The inverse relationship between pyruvate kinase activity and the percentage of modified peptides observed suggests that the accumulation of adducts on a variety of residues contributes to conformational change in the protein leading to major loss of activity, although the possibility that increasing extent of modification on a single residue is responsible cannot be discounted. As losses in activity were observed at 38 μM acrolein and HHE after 10 min and 10 μM after 4 h treatments, this suggests that adducts occurring with these treatment conditions on Cys 152, Cys358, Cys423, His 464, Cys474 are most likely to be involved. The absence of inhibition by short treatments with MDA despite modification of many lysines implies that none of these residues are required for activity, and may even represent surface decoys for oxidative damage. The eventual loss of activity above 1 mM MDA probably reflects conformational changes and unfolding of the protein, rather than a specific effect of individual adducts. In contrast, 2 h treatments at 100-200 μM did show slight inhibition, but corresponding adducts could not be detected. Nevertheless, lysine modifications were also observed following HHE and acrolein treatments, and lysine residues have been reported to be important in regulation of pyruvate kinase: for example, inhibition through interaction with phosphotyrosine-containing proteins occurs at Lys433 and causes release of bound F-1,6-bP [52-54]. Possibly little inhibition was observed in our study as F-1,6-bP was not included in the assay. On the other hand, crosslinking of lysine residues on enzymes has also been found to inhibit proteolysis [55].

The extractable pyruvate kinase activity in the human breast cancer cell line MCF-7 was found to be extremely susceptible to cellular acrolein treatment, with more than 80% loss of activity after 2 h of 10 μM acrolein, in contrast to an inhibition of about 30% *in vitro* with the same treatment. MDA also had a much stronger inhibitory effect on cellular pyruvate kinase, compared to the minimal effect on activity *in vitro* and also the lack of toxicity over the concentration range tested, whereas the effects of HHE *in vitro* and *in vivo* were similar. It is important to note that the effects of treatments *in vitro* and in cells cannot be directly compared, as work *in vitro* was carried out with rabbit muscle pyruvate kinase, which expresses the PKM1 isoform that is constitutively tetrameric with high activity, whereas the MCF-7 cells are known to contain mainly the PKM2 isoform [56], which is allosterically regulated and readily dissociates into dimers or monomers with lower activity. Nevertheless, it is clear that pyruvate kinase is highly susceptible to electrophilic inactivation despite the large number of potential protein targets in cells. However, it is not clear from the data obtained whether the loss of activity was due to irreversible inhibition of pyruvate kinase, increased degradation of modified enzyme, or decreased synthesis of active enzyme. A previous investigation of damage to cellular proteins by HNE and ONE using click chemistry to select modified proteins followed by shotgun proteomics identified pyruvate kinase isoforms M1, M2 and R as susceptible proteins [57], and a recent study on the same electrophilic compounds also reported that PKM2 in human colorectal carcinoma (RKO) cells was very readily modified [42], thus supporting the hypothesis that the loss of activity relates directly to pyruvate kinase modification. We also observed modifications of cellular pyruvate kinase by acrolein, on Cys152 and Cys358, which may contribute to the loss of activity.

Interestingly, for both treatments the loss of activity at low treatment concentrations was less severe after 24 h than 2 h. The most likely explanation for this phenomenon is that during the longer treatment, defence responses are activated, and cellular synthesis of the enzyme occurs, to counteract the loss of activity. In fact, pyruvate kinase has a relatively high turnover rate with half-life of 0.7 days [58], which could explain the recovery of enzyme activity at 24 h compared to the 2-h incubations at lower concentrations of aldehyde, although this turnover rate was not measured under stress conditions. It is also well established that covalent modification of cellular proteins by HNE and analogous electrophilic compounds targets them to the 20S proteasome for degradation and recycling [59], although more severe treatments that cause cross-linking via lysines as mentioned previously [55] and protein aggregation can inhibit the proteasome and ultimately lead to cell death [60].

Changes in pyruvate kinase isoforms and activity have been reported during the transformation of cells to a proliferative or tumorigenic phenotype, and have often been linked to the switch to aerobic glycolysis (the Warburg effect) [10]. This has normally been associated with increased glucose utilization and production of lactate. Oxidative modifications appear to represent another way to affect PKM2 activity and coordinate the metabolic response to altered redox balance in cancer cells. It has been suggested that inhibition of pyruvate kinase causes a backing-up of metabolites in glycolysis as far at glucose-6-phosphate, leading to an increased flux through the pentose phosphate pathway that facilitates antioxidant defence through increased formation of NADPH and maintenance of reduced glutathione pools [18]. This may involve inhibitory effects of PEP on triose phosphate isomerase, based on studies in oxidatively stressed yeast [19]. There is an apparent paradox in the fact that cancer cells manage to maintain high lactate production despite low activity of pyruvate kinase; Harris and Fenton have suggested that rather than inhibition per se, the PKM2 isoform has a high Km for PEP that results in a different steady-state flux through glycolysis with high intermediate levels that support both lactate formation and the pentose phosphate pathway [61]. However, there is clearly evidence for elevated levels of both oxidants and antioxidants in cancer [62], as well as a high susceptibility of pyruvate kinase to oxidative and electrophilic attack, both from the data presented here and previous studies [15,17,19,42]. In the case of inhibition by electrophilic species that cause covalent adduct formation, it seems likely that increased flux through the pentose phosphate pathway and altered metabolic state also allows increased protein synthesis to maintain key enzyme activities.

In summary, this study has provided novel data on the susceptibility of the key glycolytic enzyme pyruvate kinase to modification by 3 aldehydes with different chemical reactivities: acrolein (an alkenal), HHE (a hydroxyalkenal), and MDA (a dicarbonyl), and has shown that they cause differential inhibition of activity both *in vitro* and in a breast cancer cell line. Pyruvate kinase in MCF-7 cells was extremely susceptible to inhibition and modification by acrolein, which is a carcinogen present in tobacco smoke as well as a product of lipid peroxidation, thus suggesting an additional mechanism by which this compound may contribute to tumorigenesis.

Funding/Acknowledgments

This project has received funding from the European Union's Horizon 2020 research and innovation programme under the Marie Sklowdowska-Curie grant agreement number 675132 www.masstrplan.org. The data are available online at Aston Research Data Explorer https://doi.org/10.17036/researchdata.aston.ac.uk.00000415.

Appendix A. Supplementary data

Supplementary data to this article can be found online at https://doi.org/10.1016/j.freeradbiomed.2019.05.028.

Abbreviations

ACR	acrolein
F-1,6-bP	fructose-1,6-bisphosphate
FDP-lysine	N^{ε}-(3-formyl-3,4-dehydropiperidino)-lysine
DTT	dithiothreitol
ESI	electrospray ionisation
HHE	4-hydroxy-2-hexenal
HNE	4-hydroxy-2-nonenal
HPLC	high-performance liquid chromatography
IDA	Information-dependent acquisition
LC	liquid chromatography
MDA	malondialdehyde
MS	mass spectrometry
ONE	4-oxononenal
PEP	phosphoenolpyruvate
PK/PYK	pyruvate kinase
PROS	partially reduced oxygen species
PUFA	polyunsaturated fatty acid
QUAD	quadrupole
Rt	Retention time
TOF	time of flight

References

[1] O. Warburg, On the origin of cancer cells, Science 123 (1956) 309–314.
[2] M.V. Gwangwa, A.M. Joubert, M.H. Visagie, Crosstalk between the Warburg effect, redox regulation and autophagy induction in tumourigenesis, Cell. Mol. Biol. Lett. 23 (2018) 20.
[3] S.W. Kang, S. Lee, E.K. Lee, ROS and energy metabolism in cancer cells: alliance for fast growth, Arch Pharm. Res. (Seoul) 38 (2015) 338–345.
[4] V. Sosa, T. Moline, R. Somoza, R. Paciucci, H. Kondoh, L.L. ME, Oxidative stress and cancer: an overview, Ageing Res. Rev. 12 (2013) 376–390.
[5] E. Mullarky, L.C. Cantley, Diverting glycolysis to combat oxidative stress, in: K. Nakao, N. Minato, S. Uemoto (Eds.), Innovative Medicine: Basic Research and Development. Tokyo, 2015, pp. 3–23.
[6] P. Eaton, N. Wright, D.J. Hearse, M.J. Shattock, Glyceraldehyde phosphate dehydrogenase oxidation during cardiac ischemia and reperfusion, J. Mol. Cell. Cardiol. 34 (2002) 1549–1560.
[7] T. Ishii, O. Sunami, H. Nakajima, H. Nishio, T. Takeuchi, F. Hata, Critical role of sulfenic acid formation of thiols in the inactivation of glyceraldehyde-3-phosphate dehydrogenase by nitric oxide, Biochem. Pharmacol. 58 (1999) 133–143.
[8] J.M. Souza, R. Radi, Glyceraldehyde-3-phosphate dehydrogenase inactivation by peroxynitrite, Arch. Biochem. Biophys. 360 (1998) 187–194.
[9] M. Yi, Y. Ban, Y. Tan, W. Xiong, G. Li, B. Xiang, 6-Phosphofructo-2-kinase/fructose-2,6-biphosphatase 3 and 4: a pair of valves for fine-tuning of glucose metabolism in human cancer, Mol Metab 20 (2019) 1–13.
[10] W. Luo, G.L. Semenza, Emerging roles of PKM2 in cell metabolism and cancer progression, Trends Endocrinol. Metabol. 23 (2012) 560–566.
[11] H.R. Christofk, M.G. Vander Heiden, M.H. Harris, A. Ramanathan, R.E. Gerszten, R. Wei, M.D. Fleming, S.L. Schreiber, L.C. Cantley, The M2 splice isoform of pyruvate kinase is important for cancer metabolism and tumour growth, Nature 452 (2008) 230–233.
[12] K. Ashizawa, P. McPhie, K.H. Lin, S.Y. Cheng, An in vitro novel mechanism of regulating the activity of pyruvate kinase M2 by thyroid hormone and fructose 1, 6-bisphosphate, Biochemistry 30 (1991) 7105–7111.
[13] J.D. Dombrauckas, B.D. Santarsiero, A.D. Mesecar, Structural basis for tumor pyruvate kinase M2 allosteric regulation and catalysis, Biochemistry 44 (2005) 9417–9429.
[14] M.S. Jurica, A. Mesecar, P.J. Heath, W. Shi, T. Nowak, B.L. Stoddard, The allosteric regulation of pyruvate kinase by fructose-1,6-bisphosphate, Structure 6 (1998) 195–210.
[15] D. Anastasiou, G. Poulogiannis, J.M. Asara, M.B. Boxer, J.K. Jiang, M. Shen, G. Bellinger, A.T. Sasaki, J.W. Locasale, D.S. Auld, C.J. Thomas, M.G. Vander Heiden, L.C. Cantley, Inhibition of pyruvate kinase M2 by reactive oxygen species contributes to cellular antioxidant responses, Science 334 (2011) 1278–1283.
[16] B. McDonagh, S. Ogueta, G. Lasarte, C.A. Padilla, J.A. Barcena, Shotgun redox proteomics identifies specifically modified cysteines in key metabolic enzymes under oxidative stress in Saccharomyces cerevisiae, J. Proteom. 72 (2009) 677–689.
[17] A.R. Mitchell, M. Yuan, H.P. Morgan, I.W. McNae, E.A. Blackburn, T. Le Bihan, R.A. Homem, M. Yu, G.J. Loake, P.A. Michels, M.A. Wear, M.D. Walkinshaw, Redox regulation of pyruvate kinase M2 by cysteine oxidation and S-nitrosation, Biochem. J. 475 (2018) 3275–3291.
[18] S.Y. Lunt, V. Muralidhar, A.M. Hosios, W.J. Israelsen, D.Y. Gui, L. Newhouse, M. Ogrodzinski, V. Hecht, K. Xu, P.N. Acevedo, D.P. Hollern, G. Bellinger, T.L. Dayton, S. Christen, I. Elia, A.T. Dinh, G. Stephanopoulos, S.R. Manalis, M.B. Yaffe, E.R. Andrechek, S.M. Fendt, M.G. Vander Heiden, Pyruvate kinase isoform expression alters nucleotide synthesis to impact cell proliferation, Mol. Cell 57 (2015) 95–107.
[19] N.M. Gruning, M. Rinnerthaler, K. Bluemlein, M. Mulleder, M.M. Wamelink, H. Lehrach, C. Jakobs, M. Breitenbach, M. Ralser, Pyruvate kinase triggers a metabolic feedback loop that controls redox metabolism in respiring cells, Cell Metabol. 14 (2011) 415–427.
[20] E. Eigenbrodt, M. Reinacher, U. Scheefers-Borchel, H. Scheefers, R. Friis, Double role for pyruvate kinase type M2 in the expansion of phosphometabolite pools found in tumor cells, Crit. Rev. Oncog. 3 (1992) 91–115.
[21] B.C. Sousa, A.R. Pitt, C.M. Spickett, Chemistry and analysis of HNE and other prominent carbonyl-containing lipid oxidation compounds, Free Radical Biol. Med. 111 (2017) 294–308.
[22] A. Reis, C.M. Spickett, Chemistry of phospholipid oxidation, Biochim. Biophys. Acta 1818 (2012) 2374–2387.
[23] R.M. Domingues, P. Domingues, T. Melo, D. Perez-Sala, A. Reis, C.M. Spickett, Lipoxidation adducts with peptides and proteins: deleterious modifications or signaling mechanisms? J. Proteom. 92 (2013) 110–131.
[24] S. Pizzimenti, E. Ciamporcero, M. Daga, P. Pettazzoni, A. Arcaro, G. Cetrangolo, R. Minelli, C. Dianzani, A. Lepore, F. Gentile, G. Barrera, Interaction of aldehydes derived from lipid peroxidation and membrane proteins, Front. Physiol. 4 (2013) 242.
[25] G. Barrera, S. Pizzimenti, E.S. Ciamporcero, M. Daga, C. Ullio, A. Arcaro, G.P. Cetrangolo, C. Ferretti, C. Dianzani, A. Lepore, F. Gentile, Role of 4-hydroxynonenal-protein adducts in human diseases, Antioxidants Redox Signal. 22 (2015) 1681–1702.
[26] F.J. Van Kuijk, L.L. Holte, E.A. Dratz, 4-Hydroxyhexenal: a lipid peroxidation product derived from oxidized docosahexaenoic acid, Biochim. Biophys. Acta 1043 (1990) 116–118.
[27] A. Ayala, M.F. Munoz, S. Arguelles, Lipid peroxidation: production, metabolism, and signaling mechanisms of malondialdehyde and 4-hydroxy-2-nonenal, Oxid. Med. Cell. Longev. 2014 (2014) 360438.
[28] M. Khoubnasabjafari, K. Ansarin, A. Jouyban, Reliability of malondialdehyde as a biomarker of oxidative stress in psychological disorders, Bioimpacts : BI 5 (2015) 123–127.
[29] H.J. Forman, O. Augusto, R. Brigelius-Flohe, P.A. Dennery, B. Kalyanaraman, H. Ischiropoulos, G.E. Mann, R. Radi, L.J. Roberts 2nd, J. Vina, K.J. Davies, Even free radicals should follow some rules: a guide to free radical research terminology and methodology, Free Radical Biol. Med. 78 (2015) 233–235.
[30] D. Del Rio, A.J. Stewart, N. Pellegrini, A review of recent studies on malondialdehyde as toxic molecule and biological marker of oxidative stress, Nutr. Metabol. Cardiovasc. Dis. : Nutr. Metabol. Cardiovasc. Dis. 15 (2005) 316–328.
[31] D. Aizenbud, I. Aizenbud, A.Z. Reznick, K. Avezov, Acrolein-an alpha,beta-unsaturated aldehyde: a review of oral cavity exposure and oral pathology effects, Rambam Maimonides Med. J. 7 (2016).
[32] K. Uchida, M. Kanematsu, Y. Morimitsu, T. Osawa, N. Noguchi, E. Niki, Acrolein is a product of lipid peroxidation reaction. Formation of free acrolein and its conjugate with lysine residues in oxidized low density lipoproteins, J. Biol. Chem. 273 (1998) 16058–16066.
[33] J.P. Kehrer, S.S. Biswal, The molecular effects of acrolein, Toxicol. Sci. : Off. J. Soc. Toxicol. 57 (2000) 6–15.
[34] J.F. Stevens, C.S. Maier, Acrolein: sources, metabolism, and biomolecular interactions relevant to human health and disease, Mol. Nutr. Food Res. 52 (2008) 7–25.
[35] H. Zhong, H. Yin, Role of lipid peroxidation derived 4-hydroxynonenal (4-HNE) in cancer: focusing on mitochondria, Redox Biol 4 (2015) 193–199.
[36] G. Barrera, Oxidative stress and lipid peroxidation products in cancer progression and therapy, ISRN Oncol 2012 (2012) 137289.
[37] K. Uchida, E.R. Stadtman, Covalent attachment of 4-hydroxynonenal to glyceraldehyde-3-phosphate dehydrogenase. A possible involvement of intra- and intermolecular cross-linking reaction, J. Biol. Chem. 268 (1993) 6388–6393.
[38] M. Nakamura, H. Tomitori, T. Suzuki, A. Sakamoto, Y. Terui, R. Saiki, N. Dohmae, K. Igarashi, K. Kashiwagi, Inactivation of GAPDH as one mechanism of acrolein toxicity, Biochem. Biophys. Res. Commun. 430 (2013) 1265–1271.
[39] K. Igarashi, T. Uemura, K. Kashiwagi, Acrolein toxicity at advanced age: present and future, Amino Acids 50 (2018) 217–228.
[40] J. Gerszon, A. Rodacka, Oxidatively modified glyceraldehyde-3-phosphate dehydrogenase in neurodegenerative processes and the role of low molecular weight compounds in counteracting its aggregation and nuclear translocation, Ageing Res. Rev. 48 (2018) 21–31.
[41] C.J. Martyniuk, B. Fang, J.M. Koomen, T. Gavin, L. Zhang, D.S. Barber, R.M. Lopachin, Molecular mechanism of glyceraldehyde-3-phosphate dehydrogenase inactivation by alpha,beta-unsaturated carbonyl derivatives, Chem. Res. Toxicol. 24 (2011) 2302–2311.
[42] J.M. Camarillo, J.C. Ullery, K.L. Rose, L.J. Marnett, Electrophilic modification of PKM2 by 4-hydroxynonenal and 4-oxononenal results in protein cross-linking and kinase inhibition, Chem. Res. Toxicol. 30 (2017) 635–641.
[43] L. Soulere, Y. Queneau, A. Doutheau, An expeditious synthesis of 4-hydroxy-2E-nonenal (4-HNE), its dimethyl acetal and of related compounds, Chem. Phys. Lipids 150 (2007) 239–243.
[44] S. Bouzbouz, E. de Lemos, J. Cossy, J. Saez, X. Franck, B. Figadere, Natural (5′-oxoheptene-1′E,3′E-dienyl)-5,6-dihydro-2H- Pyran-2-One: Total Synthesis and

Revision of its Absolute Configuration, (2004).
[45] I. Verrastro, K. Tveen-Jensen, R. Woscholski, C.M. Spickett, A.R. Pitt, Reversible oxidation of phosphatase and tensin homolog (PTEN) alters its interactions with signaling and regulatory proteins, Free Radical Biol. Med. 90 (2016) 24–34.
[46] C.B. Afonso, B.C. Sousa, A.R. Pitt, C.M. Spickett, A mass spectrometry approach for the identification and localization of small aldehyde modifications of proteins, Arch. Biochem. Biophys. 646 (2018) 38–45.
[47] M.H. El-Maghrabey, N. Kishikawa, K. Ohyama, N. Kuroda, Analytical method for lipoperoxidation relevant reactive aldehydes in human sera by high-performance liquid chromatography-fluorescence detection, Anal. Biochem. 464 (2014) 36–42.
[48] K. Sakata, K. Kashiwagi, S. Sharmin, S. Ueda, Y. Irie, N. Murotani, K. Igarashi, Increase in putrescine, amine oxidase, and acrolein in plasma of renal failure patients, Biochem. Biophys. Res. Commun. 305 (2003) 143–149.
[49] W.J. Israelsen, M.G. Vander Heiden, Pyruvate kinase: function, regulation and role in cancer, Semin. Cell Dev. Biol. 43 (2015) 43–51.
[50] W.J. Israelsen, T.L. Dayton, S.M. Davidson, B.P. Fiske, A.M. Hosios, G. Bellinger, J. Li, Y. Yu, M. Sasaki, J.W. Horner, L.N. Burga, J. Xie, M.J. Jurczak, R.A. DePinho, C.B. Clish, T. Jacks, R.G. Kibbey, G.M. Wulf, D. Di Vizio, G.B. Mills, L.C. Cantley, M.G. Vander Heiden, PKM2 isoform-specific deletion reveals a differential requirement for pyruvate kinase in tumor cells, Cell 155 (2013) 397–409.
[51] L. Lv, D. Li, D. Zhao, R. Lin, Y. Chu, H. Zhang, Z. Zha, Y. Liu, Z. Li, Y. Xu, G. Wang, Y. Huang, Y. Xiong, K.L. Guan, Q.Y. Lei, Acetylation targets the M2 isoform of pyruvate kinase for degradation through chaperone-mediated autophagy and promotes tumor growth, Mol. Cell 42 (2011) 719–730.
[52] H.R. Christofk, M.G. Vander Heiden, N. Wu, J.M. Asara, L.C. Cantley, Pyruvate kinase M2 is a phosphotyrosine-binding protein, Nature 452 (2008) 181–186.
[53] T. Hitosugi, S. Kang, M.G. Vander Heiden, T.W. Chung, S. Elf, K. Lythgoe, S. Dong, S. Lonial, X. Wang, G.Z. Chen, J. Xie, T.L. Gu, R.D. Polakiewicz, J.L. Roesel, T.J. Boggon, F.R. Khuri, D.G. Gilliland, L.C. Cantley, J. Kaufman, J. Chen, Tyrosine phosphorylation inhibits PKM2 to promote the Warburg effect and tumor growth, Sci. Signal. 2 (2009) ra73.
[54] B. Varghese, G. Swaminathan, A. Plotnikov, C. Tzimas, N. Yang, H. Rui, S.Y. Fuchs, Prolactin inhibits activity of pyruvate kinase M2 to stimulate cell proliferation, Mol. Endocrinol. 24 (2010) 2356–2365.
[55] B. Friguet, L.I. Szweda, Inhibition of the multicatalytic proteinase (proteasome) by 4-hydroxy-2-nonenal cross-linked protein, FEBS Lett. 405 (1997) 21–25.
[56] K. Taniguchi, Y. Ito, N. Sugito, M. Kumazaki, H. Shinohara, N. Yamada, Y. Nakagawa, T. Sugiyama, M. Futamura, Y. Otsuki, K. Yoshida, K. Uchiyama, Y. Akao, Organ-specific PTB1-associated microRNAs determine expression of pyruvate kinase isoforms, Sci. Rep. 5 (2015) 8647.
[57] S.G. Codreanu, J.C. Ullery, J. Zhu, K.A. Tallman, W.N. Beavers, N.A. Porter, L.J. Marnett, B. Zhang, D.C. Liebler, Alkylation damage by lipid electrophiles targets functional protein systems, Mol. Cell. Proteom. 13 (2014) 849–859.
[58] D. Illg, D. Pette, Turnover rates of hexokinase I, phosphofructokinase, pyruvate kinase and creatine kinase in slow-twitch soleus muscle and heart of the rabbit, Eur. J. Biochem. 97 (1979) 267–273.
[59] J.P. Castro, T. Jung, T. Grune, W. Siems, 4-Hydroxynonenal (HNE) modified proteins in metabolic diseases, Free Radical Biol. Med. 111 (2017) 309–315.
[60] A. Hohn, T. Jung, T. Grune, Pathophysiological importance of aggregated damaged proteins, Free Radical Biol. Med. 71 (2014) 70–89.
[61] R.A. Harris, A.W. Fenton, A critical review of the role of M2PYK in the Warburg effect, Biochim. Biophys. Acta Rev. Canc. 1871 (2019) 225–239.
[62] A. Glasauer, N.S. Chandel, Targeting antioxidants for cancer therapy, Biochem. Pharmacol. 92 (2014) 90–101.